J Neurophysiol 100: 1523–1532, 2008.
First published June 18, 2008; doi:10.1152/jn.00076.2008.

Synchronization of Neuronal Responses in Primary Visual Cortex of Monkeys Viewing Natural Images

Pedro Maldonado,[1] Cecilia Babul,[1] Wolf Singer,[2] Eugenio Rodriguez,[2] Denise Berger,[3,4] and Sonja Grün[4,5]

[1]*Centro de Neurociencias Integradas and Programa de Fisiología y Biofísica, Facultad de Medicina, Universidad de Chile, Santiago, Chile;* [2]*Max Planck Institute for Brain Research, Frankfurt am Main;* [3]*Neuroinformatics, Institute for Biology (Neurobiology), Free University and* [4]*Bernstein Center for Computational Neuroscience, Berlin, Germany;* [5]*Theoretical Neuroscience Group, RIKEN Brain Science Institute, Saitama, Japan*

Submitted 22 January 2008; accepted in final form 12 June 2008

Maldonado P, Babul C, Singer W, Rodriguez E, Berger D, Grün S. Synchronization of neuronal responses in primary visual cortex of monkeys viewing natural images. *J Neurophysiol* 100: 1523–1532, 2008. First published June 18, 2008; doi:10.1152/jn.00076.2008. When inspecting visual scenes, primates perform on average four saccadic eye movements per second, which implies that scene segmentation, feature binding, and identification of image components is accomplished in <200 ms. Thus individual neurons can contribute only a small number of discharges for these complex computations, suggesting that information is encoded not only in the discharge rate but also in the timing of action potentials. While monkeys inspected natural scenes we registered, with multielectrodes from primary visual cortex, the discharges of simultaneously recorded neurons. Relating these signals to eye movements revealed that discharge rates peaked around 90 ms after fixation onset and then decreased to near baseline levels within 200 ms. Unitary event analysis revealed that preceding this increase in firing there was an episode of enhanced response synchronization during which discharges of spatially distributed cells coincided within 5-ms windows significantly more often than predicted by the discharge rates. This episode started 30 ms after fixation onset and ended by the time discharge rates had reached their maximum. When the animals scanned a blank screen a small change in firing rate, but no excess synchronization, was observed. The short latency of the stimulation-related synchronization phenomena suggests a fast-acting mechanism for the coordination of spike timing that may contribute to the basic operations of scene segmentation.

INTRODUCTION

When inspecting visual scenes it can be anticipated that a novel input constellation needs to be processed each time a saccadic eye movement is performed to shift the gaze to a new position. Primates perform up to four saccades per second, suggesting that feature extraction, perceptual grouping of features belonging to individual objects, and identification of objects can be accomplished within about 200 ms. Similar conclusions on processing speed have been derived from psychophysical experiments with human subjects who had to recognize individual objects in cluttered scenes (Fabre-Thorpe et al. 2001). Based on the evidence that processing can be surprisingly fast, it had further been proposed that the neuronal networks at early stages of visual processing should accomplish functions such as feature extraction, scene segmentation, and perceptual grouping by exchanging only a few spikes per neuron (Guyonneau et al. 2004). In this case, only a limited amount of information can be encoded by varying the discharge rate and it has thus been suggested that, in addition, the cortex might exploit a temporal code. In this case, information would also be encoded in the precise timing of action potentials (Fries et al. 2001, 2007; Grün et al. 2002a; Hopfield 2004). However, little is known about the responses of cells in the visual cortex when animals are free to explore natural images. In cats and monkeys, neuronal responses to stimuli placed in the cells' receptive field (RF) are modified by stimuli presented outside the "classical" RF (Jones et al. 2001; McAdams et al. 1999; Sugita 1999; Trotter et al. 1999). Recent studies in monkeys exposed to complex visual stimuli that simulate natural viewing conditions have shown, in addition, that neurons in the primary visual cortex (V1) significantly reduce their firing when a larger portion of the visual field is covered with the sample image (Vinje et al. 2000). These context-dependent modulatory processes have been hypothesized to participate in stimulus selection, scene segmentation, and perceptual grouping. However, little is known about how these multiple modulatory influences combine when animals are allowed to freely scan visual scenes and no data are available on precise timing relations among the discharges of simultaneously recorded neurons. We hypothesized that information is encoded not only in discharge rates but also in timing relations among the spikes of individual neurons; thus we should find indications of precise timing, e.g., synchronization of discharges in these data.

Using an array of eight individually adjustable tetrodes we simultaneously recorded the discharges of multiple neurons from the V1 of two adult, male capuchin monkeys (*Cebus apella*). The animals were presented with a collection of pictures of different natural scenes. Using Unitary Event (UE) analysis, we demonstrate an increased and highly precise spike synchronization that is dissociated from the later increase in neuronal firing rate. These results suggest that coordination of the timing of discharges may play an important role in the initial processing of signals in V1.

METHODS

Subjects and recording setup

All experiments followed institutional and National Institutes of Health guidelines for the care and use of laboratory animals. Two adult, male capuchin monkeys (*Cebus apella*) weighing 3–4 kg

Address for reprint requests and other correspondence: P. E. Maldonado, Universidad de Chile, Programa de Fisiología y Biofísica, Facultad de Medicina, Casilla 70005, Santiago, Chile (E-mail: pedro@neuro.med.uchile.cl).

The costs of publication of this article were defrayed in part by the payment of page charges. The article must therefore be hereby marked "*advertisement*" in accordance with 18 U.S.C. Section 1734 solely to indicate this fact.

served as subjects for this study. All surgical and recording procedures were similar to those in Friedman-Hill et al. (2000). A hard plastic recording chamber with eight independently movable nichrome tetrodes was mounted over the surface of the V1. Guiding tubes were positioned on top of the dura mater. Tetrodes could be lowered ≤3–4 mm; thus we could record from the top cortex as well as a second section of V1 located underneath. After the end of recordings, the head post, eye coils, and manipulator were removed and after full recovery the animals were donated for adoption.

Visual task and eye movements

The animals were seated in a chamber dimly lit at the low scotopic level and presented with a collection of 15 pictures of different natural scenes that were displayed on a 21-in. computer monitor (frame rate 60 Hz) located 57 cm in front of the animals, subtending 30 × 40° of visual angle. Each image was presented at least three times in a single recording session. The animals were allowed to freely explore natural images ("images") or black frames ("blank"). The experimental protocol required the animals to maintain their gaze for ≤5 s within the limits of the frames, to be rewarded with a drop of juice. To maintain alertness, we also presented black frames that contained a single central fixation spot that the animals had to fixate for 1 s to be rewarded (1° window). Vertical and horizontal eye positions were monitored with a search coil driver (DNI Instruments; resolution: 1.2 min of arc) by magnetic induction of an implanted coil (Judge et al. 1980) and then digitized at 2 kHz (see Fig. 1). Eye coils were made of three loops of Teflon-coated wire and implanted over the sclera, one in each eye. Eye coils were calibrated using fixation points located at nine different positions on the screen. The calibration procedure was performed at the beginning of each recording session.

Recordings

Neuronal activity of neighboring neurons was recorded with an array of eight individually adjustable custom-fabricated nichrome tetrodes (1- to 2-MΩ impedance). The tetrode wires were 12 μm thick made of nickel chromium (Kanthal, Palm Coast, FL), insulated with polyamide, and wound together in a four-wire array. The tetrodes were mounted in a 33G stainless-still tubing, which was beveled in a grinding wheel and gold plated (for construction details, see Gray et al. 1995). The tetrodes were positioned in a circular array, with a center-to-center distance of about 400 μm. The signals were amplified (×10K), band-pass filtered for single-unit activity (0.5–5 kHz), sampled at 25 kHz, and then stored for off-line spike sorting and analysis. Signals were fed through an off-line sorting program to reconstruct the spike trains of units recorded simultaneously by a single tetrode. Since the tetrode array remained in the animals for several days, each successive recording through the same penetration was resumed always ≥200 μm deeper than that during the previous session. This sampling procedure was continued until activity could no longer be measured after which the guide tubes were repositioned. Some penetrations crossed V1 twice in the anterior part of the calcarine sulcus, which led to systematic changes in RF position.

Data analysis

EYE MOVEMENTS. An automatic algorithm was developed to extract from the eye traces the different types of eye movements. Saccades were defined as eye movements with an angular velocity >100°/s lasting for ≥5 ms. In addition, saccades were required to exhibit a minimum acceleration of 170°/s^2. The animals performed saccades with peak velocities that ranged between 100 and >1,000°/s; the average peak velocity was around 400°/s. Fixation periods were classified as such when they lasted ≥100 ms with the eye position maintained within 1° of the gaze location reached at the end of a saccade. To minimize errors, only pairs of unambiguous saccade-fixation sequences were considered for further analysis. The significance of firing rate changes during saccades was assessed by comparing the rates in the first 20 ms and the consecutive 20 ms following

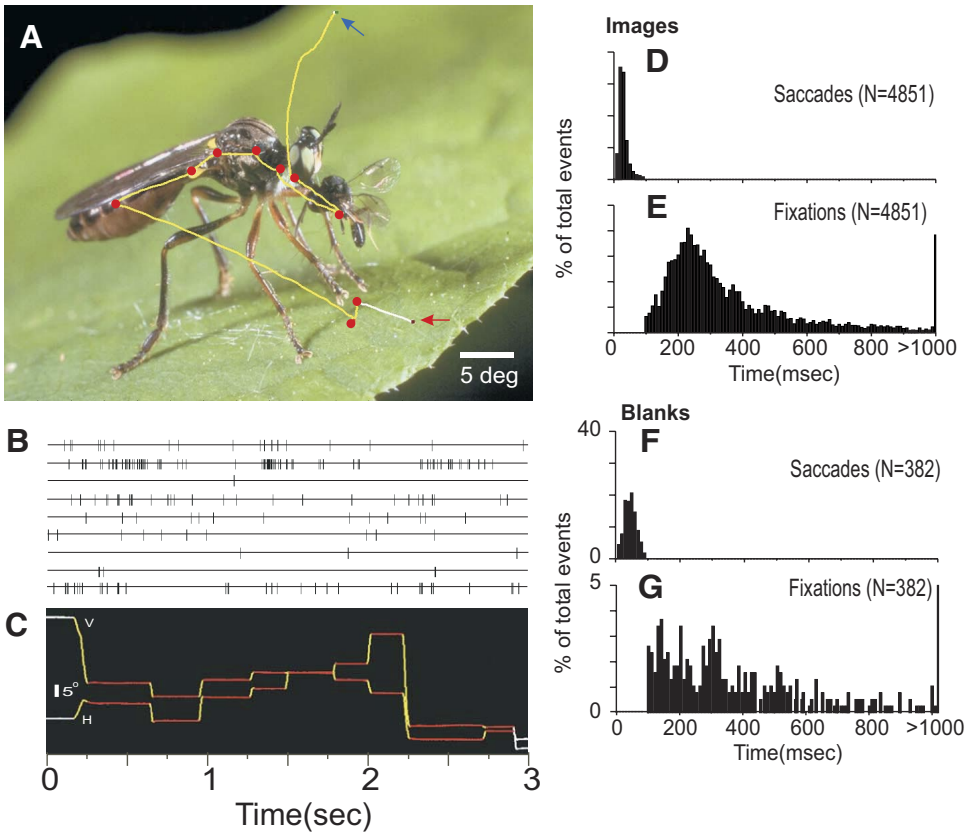

FIG. 1. Responses of cells in the primary visual cortex of a monkey (*Cebus apella*) visually exploring a natural scene. *A*: example of the presented images. Monkeys scanned the picture for ≤5 s. In this image presentation of 3-s duration, the colored line represents the eye trajectory. The yellow traces represent the saccades, the red blobs represent the fixations, and the white traces the unclassified eye movements. The blue and red arrows show the initial and final positions, respectively. *B*: spike trains from 10 simultaneously recorded cells for the time period shown in *A*. Each spike is represented as a small vertical line. Note the diversity of activity for each visual fixation shown in *C*. *C*: vertical and horizontal eye traces recorded during the same image presentation, showing the automated eye classification assignments: yellow and red for saccades and fixation, respectively. The white traces correspond to uncompleted or unclassified eye movements. *D–G*: frequency distributions of the duration of different eye movements in image (*D–E*) and blank (*F–G*) conditions, respectively. Data are from 1,219 images and 547 blank frames. Total numbers of the respective eye movements are shown in parentheses. The distributions for both saccades and fixations events differ significantly between the image and blank conditions (Kolmogorov–Smirnov, $P < 0.001$).

the onset of saccades. Significance tests for rate changes during fixations were performed comparing the first and consecutive 50 ms after the onset of the events (*t*-test).

In this study animals freely directed their visual behavior. Thus after each saccade, cells were stimulated by different portions of the image. The data thus reflect the average responses of large numbers of cells to a large number of different stimuli. We address each individual eye-movement–related event (saccade and fixation) as a "trial" and the measurement period during which electrode positions were kept constant and the constellation of recorded cells was stable as "recording session." Trials of the same event (saccades or fixations) were analyzed individually. Subsequently those occurring during the same viewing condition (image or blank) and within the same recording session were grouped. In Fig. 2*A* we illustrate the segmentation of the data from a single image presentation into trials. Since statistical analysis requires that trials have the same duration, we segmented the data using the onset of an eye-movement–related event as reference (see histograms in Fig. 1). For fixations, data were included from −25 ms before fixation onset to 325 ms after fixation onset. This epoch was chosen so that the UE analysis performed in sliding windows of 50 ms renders its first value at fixation onset. If fixations were shorter, data from subsequent eye events were included to complete the time window. An alternative would have been to include only the data from within the trial that, however, would lead to a successive decrease of data for increasing fixation duration. This in turn would lead to an increase in the noise. Therefore we decided to include data from subsequent eye events. This probably introduced distortions toward the end of the analysis window beyond 200 ms, but as the data show, the important events on which our conclusions are based all occurred within the first 100 ms after fixation onset. For the analysis of signals related to saccades, data were included from −25 to 75 ms.

ANALYSIS OF SPIKE CORRELATION. For the evaluation of temporal correlations between spikes from different neurons we used the UE analysis, a statistical method that detects the presence of spike coincidences that exceed the level predicted by the respective firing rates and evaluates their statistical significance (see METHODS; Grün et al. 1999, 2002 a,b, 2003; Riehle et al. 1997). Coincident firing that exceed the chance level by a significant amount are called *unitary events* (Grün et al. 2002a). Although in principle the method is able to handle correlations between more than two neurons, we restricted the analysis here to pairwise correlations. The reason is that the analysis of triplet coincidences or even higher complex synchrony patterns requires a higher number of samples to obtain reliable statistics. Since we are interested in the dynamics of synchrony we use a sliding-window analysis. The width of the window has to be chosen relatively small here (50 ms) to account for the changes in the firing rate. Given these constraints we decided to restrict the analysis to pairs of neurons only.

Spike trains of a pair of neurons recorded simultaneously during a particular trial were aligned to the onset of the respective event (Fig. 2*B*, "EV," here chosen as fixation onset). To account for the nonstationarity of the neurons' firing rates, the data were analyzed with a sliding window (Grün et al. 2002b). An analysis window of fixed duration T_w (here: 50 ms; gray box in Fig. 2*B*) was slid along the data such that all data are covered from the beginning to the end of the trial. The window was advanced in steps corresponding to the time resolution h of the data (0.1 ms). The first window position was centered at $t = t_0 = T_w/2$ from trial onset and the last window around time $T_w/2$ before the end of the trial. At each position of the window all the data

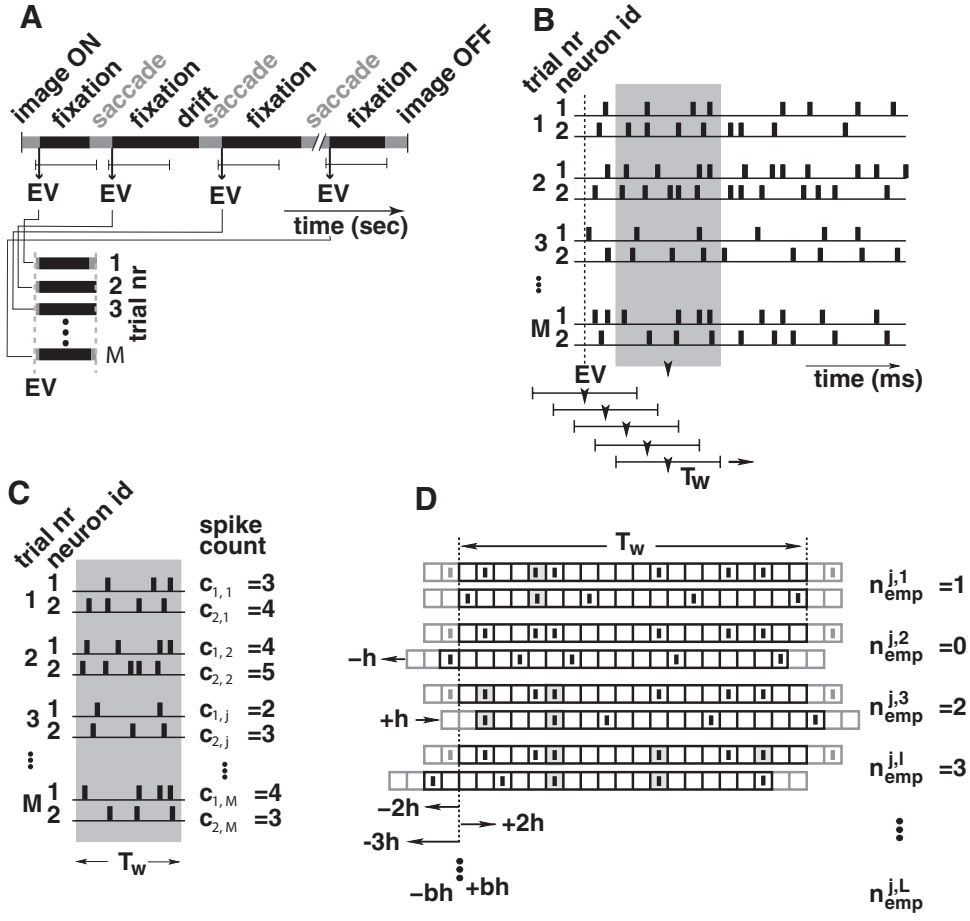

FIG. 2. Unitary event (UE) analysis. *A*: trial alignment and sliding window approach. The simultaneous spike trains of 2 neurons are aligned according to the relevant behavioral event (EV, exemplified for fixations). The data extracted in relation to such an event were from −25 ms before until 325 ms after the event. For analysis we applied a sliding window T_w (width 50 ms) that was slid along the data in the time resolution of the data of 0.1 ms. At each position of the window the UE analysis was newly performed. *B*: analysis within a window. Per trial j and per neuron i the number of spikes $c_{i,j}$ within the window is extracted. From these the data firing probabilities per trial per neuron are calculated by dividing the spike counts by the number of bins N in the window (here: 500 bins of h = 0.1 ms). These probabilities then serve to calculate the expected number of coincidences. *C*: extracting the empirical number of coincidences in a single trial. Within a single trial the number of coincidences is extracted as the joint spike events of the 2 neurons occurring within the same bin (of 0.1 ms) (marked in light gray). *D*: to also detect coincidences with small temporal jitter, the spike trains are shifted against each other in units of the bins, with increasing shift. One neuron is kept fixed as a reference, whereas the spike train of the other is shifted forward and backward up to the maximal allowed jitter b (here 5 ms). The total number of coincidences within the trial is then given by the sum of all $L = 2(b/h) + 1$ individual shifts. For simplicity we omitted the time indices of the window positions in the figures.

within the window were analyzed for unitary events and the analysis was repeated sequentially for the next positions $t_k = t_0 + kh$, where k is the index of the window positions. The results obtained for a given window position were plotted at the time point corresponding to the center of the windows (Fig. 2*B*, indicated by arrows) to obtain time-dependent measures of UEs.

The basic operation in the UE method is to compare the empirical number of coincidences to the expected number that would occur by chance given the firing rates of the neurons. Additionally, to account for nonstationary rates across trials (Grün et al. 2003), as are typically present in data of awake behaving animals and in particular in the data treated here, the relevant measures are obtained from single-trial analysis and only subsequently summed across trials. Thus within the analysis window the expected number of coincidences is calculated on the basis of the trial-by-trial firing probabilities $p_{i,j}$, which are estimated by the spike count $c_{i,j}$ of neuron i in trial j divided by the number of bins N within a window: $p_{i,j} = c_{i,j}/N$, where $N = T_w/h$ (Fig. 2*C*). The joint probability for finding a coincidence by chance per trial is calculated by the product of the single-neuron firing probabilities $p_{1,j} \cdot p_{2,j}$. The expected number of coincidences per trial j results from multiplying this probability with the number of bins N that are included in the analysis window: $n^j_{\text{exp}} = p_{1,j} \cdot p_{2,j} \cdot N$. The total number of expected coincidences within the window is derived from the sum of the expected numbers per trial: $n_{\text{exp}} = \sum_{j=1}^{M} n^j_{\text{exp}}$.

The total empirical number of coincidences per window is derived simply by counting the coincident events (spikes of both neurons within the same bin of width h) within a trial and taking the sum across all the trials. However, being interested in detecting coincidences that may occur with a small temporal jitter (e.g., up to $b = 5$ ms), we applied the "multiple-shift" approach (Grün et al. 1999). In this method the coincidences within a single trial are detected by shifting the second spike train against the first (reference) spike train (see Fig. 2*D*). The shift is stepwise increased from 0 in steps of $h = 0.1$ ms up to $b = 5$ ms (for positive and negative shifts). For each shift l of the $L = 2(b/h) + 1$ shifts, the exact coincidences $n^{j,l}_{\text{emp}}$ are counted. The total number of coincidences considering all shifts then yields the total number of empirical coincidences in that trial

$$n^j_{\text{emp}} = \sum_{l=1}^{L} n^{j,l}_{\text{emp}}$$

(Fig. 2*D*). The total sum of the empirical coincidences in a window is then given by the sum of all coincidences across the trials

$$n_{\text{emp}} = \sum_{j=1}^{M} n^j_{\text{emp}}$$

Finally, we compared the empirical n_{emp} to the expected number n_{exp} of coincidences to detect significant deviations. To this end, we calculated the joint-p-value jp [i.e., the probability of getting the given number of empirical coincidences (or an even larger number) under the null hypothesis of independent firing]. The distribution that represents the probability to find a given number of coincidences under this null hypothesis is given analytically for the case of Poisson processes. Then the coincidence counts follow a Poisson distribution, with its mean corresponding to the expected number of coincidences (for the analytical derivation see Grün et al. 2002a). (See also the discussion on deviation from the Poisson assumption in *Controls* in RESULTS.) Then the significance of n_{emp}, given n_{exp}, measured as the joint-p-value, yields (Grün et al. 2002a)

$$jp(n_{\text{emp}}, n_{\text{exp}}) = \sum_{r=n_{\text{emp}}}^{\infty} \frac{n^r_{\text{exp}}}{r!} \exp(-n_{\text{exp}})$$

If its value is below an a priori threshold (here chosen as 5%) coincident firing (synchrony) is classified as significant and the unitary events identified in this way are expressed as unitary event rate in a particular window. For better visualization of the significance values (see Fig. 3*D*) we use a log-transformed measure known as the *joint-surprise* (Grün et al. 2002a). In summary, for each window position we calculate the expected number of coincidences, the empirical number of coincidences, and the unitary events, all expressed as rates, thus obtaining time-dependent functions of the respective measures: $n_{\text{emp}}(t)$, $n_{\text{exp}}(t)$, and $UE(t)$. The described analysis was performed for each pair of simultaneously recorded neurons and separately for each session. To derive population statistics, the time-dependent functions were averaged across all neuron pairs for a particular type of trials (fixations or saccades). This yielded the average coincidence rates (expected and empirical) and the average UE rate as functions of time. An example of a UE analysis for a single pair is shown in Fig. 3.

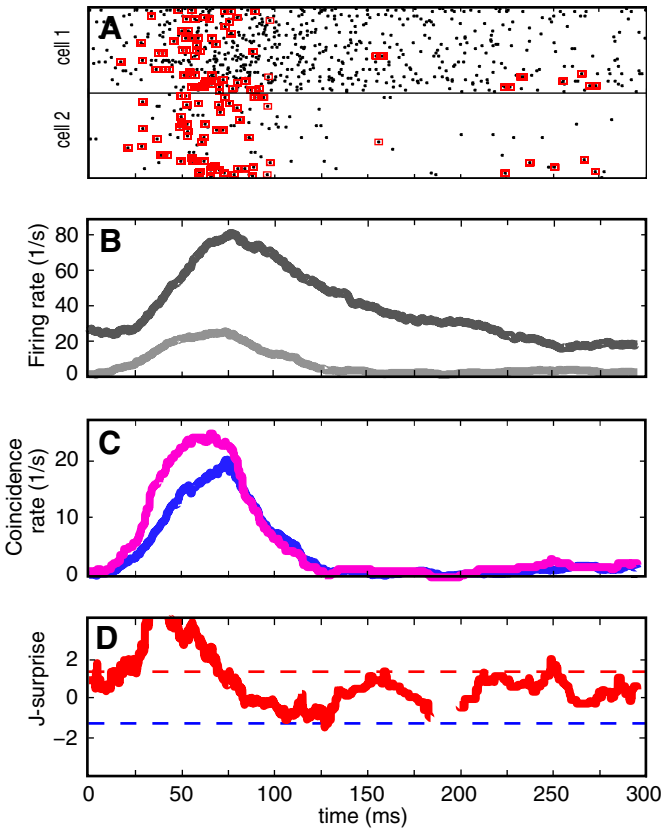

FIG. 3. Example of pairwise UE analysis. *A*: raster plots of spike responses to 57 fixations on images of cell 1 and cell 2 recorded simultaneously. *Time 0* represents the onset of fixation. Red squares indicate unitary events. UE analysis was performed within sliding windows of $T_w = 50$ ms. *B*: smoothed poststimulus time histograms (boxcar with a window of the same width as used for UE analysis) of cell 1 (dark gray) and cell 2 (light gray). *C*: expected number of coincidences (blue) and empirical number of coincidences (pink) expressed as rates. There are many more coincidences than expected at the rising phase of the firing rate response. *D*: significance of UEs expressed by the surprise measure. The surprise is not shown for values of $-\infty$ for windows in which one neuron does not have any spikes (i.e., 180–200 ms). Dashed lines correspond to a significance level of 5% (used here for UE detection): red for excess coincidences, blue for lacking coincidences.

RESULTS

Eye movements during free viewing

During free viewing of natural images, the animals performed eye movements that were categorized in saccades or fixation periods. Figure 1, *A–C* shows one example of the

presented visual scenes together with single-unit responses and the corresponding eye-movement traces. We first examined distributions of the various eye movements for all "image" and "blank" conditions. These distributions differed markedly in the two conditions (compare Fig. 1, *D* and *E* with Fig. 1, *F* and *G*). With images, saccades and fixation periods occurred typically every 250–300 ms, about sixfold more frequently than during the scanning of blank frames. Saccades were significantly longer during the blank condition than during the image condition and fixation times were scattered more broadly (Kolmogorov–Smirnov, $P < 0.001$). The distribution of the fixation durations in the image condition shows a clear peak at 230 ms, with 57% of fixations lasting between 150 and 350 ms. The corresponding distribution in the blank condition is more dispersed and fixation times are longer.

Firing rates during free viewing

We simultaneously recorded one to three cells per tetrode with at least eight tetrodes and analyzed 418 single units, individually identified by a manual clustering method (Gray et al. 1995). The receptive fields (RFs) of most units were located within 5–10° from the center of gaze and were <2°. About 15% of the recordings were made below the opercular layer. The RFs of these cells were located within 15° and their sizes were <5°. We pooled the cells from these two regions of V1 because we assumed that there are no basic differences in firing statistics. No further RF properties were determined to save time for data acquisition during free viewing.

The significance of firing rate changes during saccades was assessed by comparing the rates in the first 20 ms after the onset of saccades with those in the subsequent 20-ms interval using a *t*-test ($P < 0.05$). For fixation we compared the first 50-ms interval with the consecutive 50-ms interval after the onset of the event. In the image condition, 30% of the cells significantly increased their firing rate (Table 1) during the fixation periods and 23% of the cells significantly decreased their firing during saccades. In the blank condition significant rate changes occurred in <2% of the cells (Table 1). We examined the time course of the firing rate changes for all units by computing averaged histograms (1-ms bin width) using the onset of saccades or fixations as trigger. Given that each saccade or fixation had a different duration, each rate point (bin) is expressed as the average over the entire sample of recorded neurons, normalized to the number of neurons and trials contributing to that bin. The plots are truncated at time points beyond which <90% of the neurons contributed to the averages. Figure 4*A* summarizes the results for the image condition. Whenever the animals fixate, average firing rates increase, with a peak at about 90 ms after fixation onset, and then steadily decrease despite ongoing visual fixation. In the grand average, saccadic eye movements were associated with a decrease in firing rate consistent with saccadic suppression (Burr et al. 1994). In the blank condition (Fig. 4*B*) all changes in firing rate started from a lower baseline level than that in the image condition. Fixation periods were associated with an increment in firing rate that was smaller and developed more slowly and was more sustained than that in the image condition. This modulation of firing rate is most likely due to corollary attention-related activity associated with eye movements (Buisseret et al. 1977; Purpura et al. 2003). However, these changes were significant in only 4 of 418 single units. Saccadic eye movements were not associated with modulations in rate. During fixation of a single fixation spot displayed on an otherwise blank screen, firing rates increased rapidly toward a level corresponding to baseline activity in the image condition and then decayed slowly. This increase was significant in only 2% of the neurons. In this case measurements were triggered when the axis of gaze entered the fixation box (1°). Thus the first window contains activity associated with the end of the saccade preceding the fixation.

Temporal relations among the discharges of simultaneously recorded cells (UE analysis)

We hypothesized that rate codes are complemented by a temporal coding strategy and analyzed the data for coordination of spike timing among the discharges of simultaneously recorded neurons. Therefore we examined correlations between the firing patterns of 1,369 cell pairs that were obtained in 80 recording sessions with ≤12 simultaneously registered neurons. Altogether, 4,851 trials were analyzed with images and 383 in the blank condition. For correlation analysis we examined responses during the first 50 and 300 ms following the onset of saccades and fixations, respectively. Because of the variable duration of these eye events, these interval durations were chosen to get a reasonable number of trials for reliable statistics (see METHODS). The estimation of temporal

TABLE 1. *Summary statistics of the full data set*

	Changes in Firing Rate (Percentage of Cells, $n = 418$)			Incidence of Synchronous Firing (Percentage of Total Pairs, $n = 1{,}369$)
	A	B	C	D
	Increase	Decrease	No Change	Unitary Events
Cue fixation	1.4	1.2	97.4	21.3
Image saccades	0.4	23.2	76.4	10.8
Image fixations	30.4	0.2	69.4	34.0
Blank saccades	0.2	1.4	98.4	0.4
Blank fixations	0.7	0.2	99.1	5.0

A–C: percentage of cells showing significant changes in firing rates during the the different phases of scene inspection. The significance of changes during saccades was assessed by comparing the rates in the first 20 ms and the consecutive 20 ms following the onset of saccades and for fixations by comparing the first and consecutive 50 ms after the onset of the respective events (*t*-test). Positive or negative differences were classified as increments and decrements, respectively. D: percentage of cell pairs showing UEs in the intervals from 20 to 50 ms (saccades) and 50 to 100 ms (fixations) after the onset of the respective events.

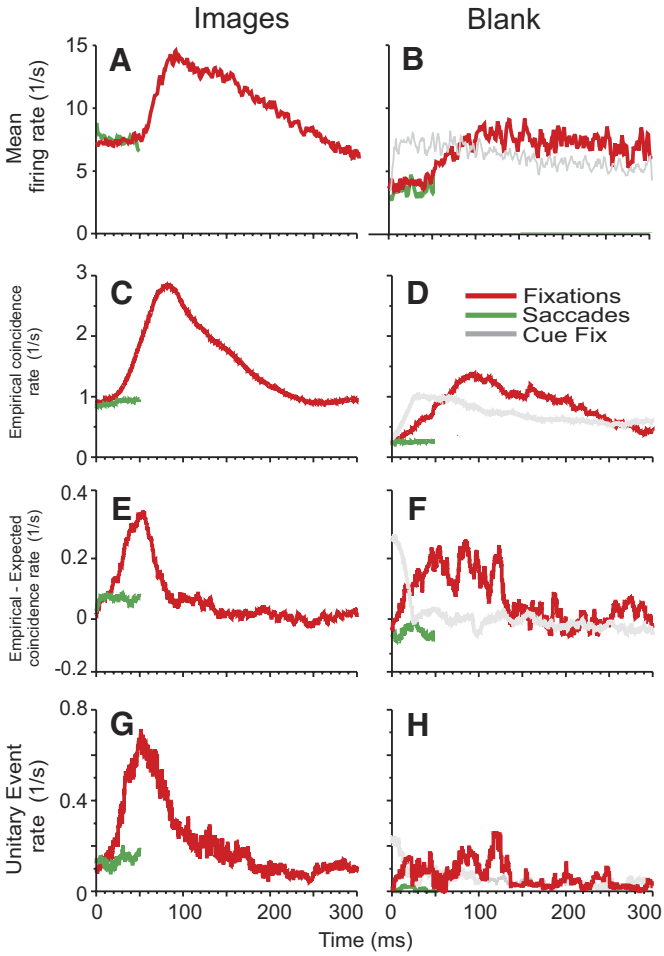

FIG. 4. Time course of changes in firing rates and synchrony associated with different eye movements. Plots are color coded (see *D*) for images (*left column*) and blank condition (*right column*). The gray lines in the *right column* refer to the condition where the animals saccade toward and fixate a central spot on an otherwise blank screen. In this condition the cells' receptive fields (RFs) fall on the dark screen. Traces for saccades are shorter than those for fixations because of the inherently shorter duration of these events. *A* and *B*: firing rates computed for and averaged over 418 single units. For each 1-ms bin, the averaged rate is computed by normalizing to the number of contributing neurons and to the corresponding number of trials per neuron. Abscissa: time from onset of saccades and fixations. *C* and *D*: frequency of empirical coincidences, defined as pairwise joint firing within 5-ms intervals computed from 1,369 simultaneously recorded cell pairs. *E* and *F*: difference of the empirically observed and the expected coincidence rates, the latter being derived from the corresponding firing rates. *G* and *H*: occurrence of unitary events (UEs), i.e., events of joint firing that significantly exceed (5%) the level of coincident firing expected from the firing rates (Grün et al. 1999, 2002a,b, 2003).

relations among the spikes of simultaneously recorded neurons becomes difficult when discharge rates are low and highly nonstationary, as is the case during the inspection of complex scenes. Therefore we used the UE analysis. Here, we address correlated firing as unitary events if the discharges of two neurons coincide within a window of 5 ms and if these coincidences significantly exceed what is predicted by the actual firing rates. To account for nonstationary firing rates, comparisons are computed between the observed (empirical) number of coincidences and the expected number of coincidences within a sliding window (here: 50 ms wide) that is moved in 0.1-ms steps along the time series. In addition, possible nonstationarities of firing rates across the trials are controlled for by estimating the firing rates and the resulting expected joint-probabilities on a trial-by-trial basis within the sliding windows.

Table 1 (under heading D) shows the incidence of UEs, i.e., of coincident firing that significantly exceeds expected levels for all cell pairs. During fixation on images, >34% of all cell pairs (n = 1,369) exhibited UEs. During cue fixations and saccades on images, 21 and 10% of all pairs showed UEs, respectively, but the mean rate of UEs was much lower than that during fixations on images (see Fig. 4*H*). In all other viewing conditions the percentage of cell pairs showing UEs was <6% and thus does not exceed the chosen level of significance (5%). The eye-movement–related time courses of the observed coincidences and UEs, averaged over all cell pairs, are shown for the image condition in Fig. 4, *G* and *H*. As expected, coincidences increase with firing rate but the precise time courses of the respective increases differ (compare Fig. 4, *A* and *G*). The reason is that there is significantly more coincident firing than expected from the respective rates during the early response phase. As the time course of the UEs indicates, this excess synchronization of firing is transient, lasts for only about 40 ms, reaches a maximum already 50 ms after onset of fixation (Fig. 4*G*), and decreases before the firing rates reach their maximum. This excess synchronization is so marked that it is already clearly visible in the difference between the observed coincidences and the coincidences predicted by the actual firing rates (Fig. 4, *E* and *F*). In the condition "fixation on blank" (Fig. 4, *B*, *D*, *F*, and *H*), the observed coincidences are slightly higher than expected from the rates (Fig. 4*F*), although this increase is not significant (Fig. 4*H*).

Controls

It can be argued that synchronous events are particularly likely if firing rates increase jointly and abruptly, as occurs in response to rapidly changing stimuli. We examined this issue by intentionally destroying the exact timing of spikes while keeping the firing rate profiles approximately constant. This is achieved by creating surrogate data by "dithering" each individual original spike of each of the neurons within a given window around the spike and reanalyzing the newly generated parallel time series in exactly the same way as the original data. Similar approaches are described in Date et al. (1998), Gerstein (2004), and Shmiel et al. (2006). As dithering width was increased from 0 to ±50 ms (centered at spike times), the maxima of the difference curves between observed and expected coincidences decreased considerably (Fig. 5*D*). Accordingly, the UE rate dropped to about 75% at ±5 ms, to 50% at ±10 ms, and approximated the level expected in the case of independent firing at about ±40 ms (Fig. 5*E*). This decay rate corresponds exactly to theoretical predictions derived for empirical coincidences that are successively dithered under consideration of the size of the coincidence window and the temporal jitter of the coincidences, indicating that the UEs were not due to transient rate covariations but are indications of excess synchrony (Pazienti et al. 2007, 2008). Pazienti et al. (2008) showed that without the presence of excess synchrony there would be no decay at all.

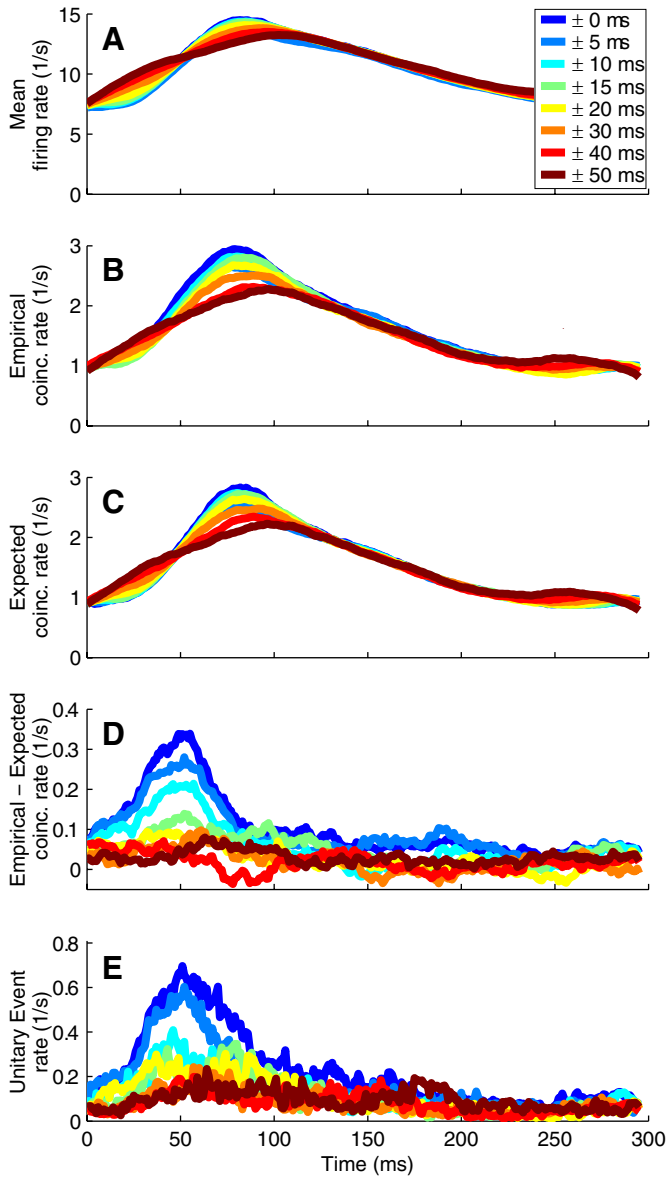

FIG. 5. Decreased synchronization with increasing dithering of spike times. Dithering was applied to each individual spike of all data and the dithered time series were analyzed for UEs as the original data (same parameters as in Fig. 3, i.e., coincidence width, 5 ms; sliding window width, 50 ms; here: shown for alignment relative to fixation onset only). Dither values varied from ±5 to ±20 ms in 10-ms steps, and from ±30 to ±50 ms in 20-ms steps (color code in *C*). *A*: average firing rates of all analyzed neurons. Abscissa (for all plots): time from onset of fixations. *B*: frequency of empirical and (*C*) expected coincidences. *D*: difference of the empirical and the expected coincidences. *E*: significant coincidences/Unitary Events. Note that dithering does not destroy all of the original coincidences. These remaining coincidences depend on the ratio of the bin width (here 5 ms) over the dither width.

Unavoidably, the firing rate profiles were also affected by the dithering and got smoothed with increasing dither (Fig. 5*A*). As a consequence, the time course of the expected coincidences was also affected (Fig. 5*C*). However, the effect of dithering was much more pronounced for the observed than for the predicted coincidences. Dithering completely abolished the peak of observed coincidences around 50 ms after fixation onset. Thus dithering is effective only on coincidences, which the UE analysis had identified as nonspurious, thereby supporting the interpretation that the UEs arise from active synchronizing processes.

To further corroborate this interpretation, we simulated spike trains that were either completely independent or contained a known number of deliberately inserted coincident spikes and then analyzed the data in exactly the same way as the experimental data. To test whether the nonstationary rate profile of the experimental data (Fig. 6*B*, gray) was causing a UE rate profile similar to that of the experimental data (Fig. 6*A*) we simulated pairs of inhomogeneous Poisson spike trains with a firing rate profile that was identical to that of the original data (Fig. 6*B*, gray). Thus these data included a possible source for false-positive correlations, i.e., covariation of firing rate

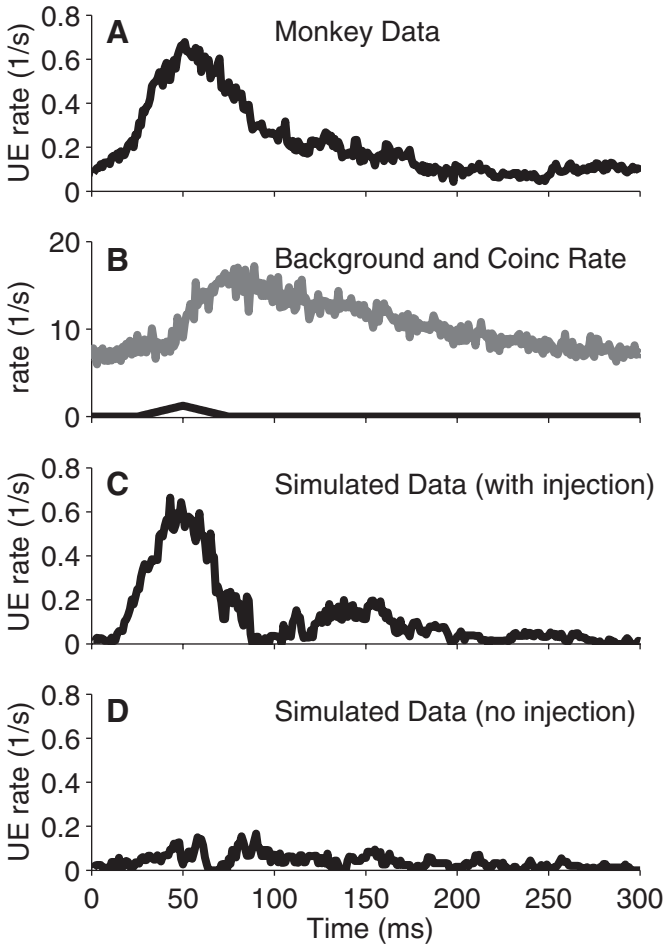

FIG. 6. Comparison of real and simulated data. *A*: UE rate of the experimental data during fixation aligned to fixation onset (as also shown in Fig. 3). *B*: firing and coincidence rate profile used for the simulation. The gray curve shows the average firing rate of all neurons (1-ms resolution). This firing rate profile is then used in the simulations. For the case of independent neurons (*D*), this time course is directly used to simulate inhomogeneous Poisson spike trains. For dependent neurons (*C*), the firing of the simulated neurons is composed of independent firing (background firing rate) and injected coincidences at a rate corresponding to the profile shown in *B* (black). In the case of injection of coincident spikes, the background firing rate was reduced by the coincidence rate such that the neurons again had the same total rate as that in the independent case. Each neuron was drawn with the same rate profile and one neuron pair was simulated for 100 trials. Coincidences were inserted with a temporal jitter of 5 ms. In all, 100 neuron pairs were simulated and then analyzed in the same way as the experimental data (sliding window of 50 ms, allowed coincidence width of 5 ms). Time course of the UE rates of the simulated data with (*C*) and without (*D*) coincidence injection.

(Grün et al. 2003). We generated a data set for 100 pairs of neurons and 100 trials per pair. For the independent spike trains, the resulting UE rate (averaged over all pairs) (Fig. 6*D*) shows no distinct peak and fluctuates around the low level expected from the 5% significance threshold. In contrast, when we injected additional coincident spikes (with a coincidence rate profile shown in Fig. 6*B*, black) and reduced the background rate such that the total rate and the rate profile of the neurons remained the same as those in the previous simulation, a prominent peak of UEs was detected. The choice for the time course of the coincidence rate was based on one of our theoretical studies in which we tested the detectability of intervals that included coincidences (Grün et al. 2002b).

We assumed Poisson statistics in the UE analysis, although being aware of the fact that experimental spike trains typically deviate from that assumption. In the study of Pipa et al. (2008) we showed that the spike train autostructure indeed has an impact on the significance estimation of coincident spike events. We specifically tested for spike trains with interspike interval (ISI) statistics given by a gamma-distribution and systematically varied the shape factor of the ISI distribution, thereby modifying spike trains from highly irregular to increasingly more regular firing. We found the false-positive rate to be at or below the expected level, given the a priori significance level for realistically regular spike trains (coefficient of variation values ranging from 0.2 to 0.8; Nawrot et al. 2008). Only for unrealistically regular or highly irregular spike trains is the false-positive rate slightly enhanced. Thus if spike trains are more regular than Poisson, the significance test assuming Poisson statistics rather underestimates the significance. To test whether our result of excess synchrony was not a result of false positives in the case of spike trains more irregular than Poisson (e.g., as given by bursty processes), we performed an additional control. We debursted the data, by excluding spikes that occurred within a time interval of <5 ms after a former spike and reanalyzed the data again. Although in some data sets the firing rate was considerably reduced, the occurrence and the time course of the UEs, as shown for the original data, were preserved (not shown here). An alternative of the significance test—based on an analytical description of the coincidence distribution for such processes—is not known and hard to derive (see Pipa et al. 2008). Generating the coincidence distribution by surrogate data is prone to errors: trial shuffling is not appropriate due to cross-trial nonstationarity, ISI shuffling would destroy potential second-order structures within the spike trains, and other methods would affect the firing rates.

Grün et al. (2002b) showed that by varying the width of the analysis window it is possible to detect the existence and the width of the interval over which coincident spikes were present. For analysis window sizes smaller that the interval of coincidences, not all coincidences are detected and the UEs are underestimated. At the width of the window that matches the interval of excess coincidences the significance curve exhibits a peak and saturates for even larger windows. The center of the maximum always stays at the same time. This is also evident in the data presented here (Fig. 7). By varying the width of the analysis window from 20 to 60 ms we always found a maximum at 50 ms after fixation, with a tendency of saturation after a width of 50 ms. This implies that regardless of the width of the analysis window, the method reliably detects the time course of nonspurious coincidences that seem to be spread over an interval of about 50 ms.

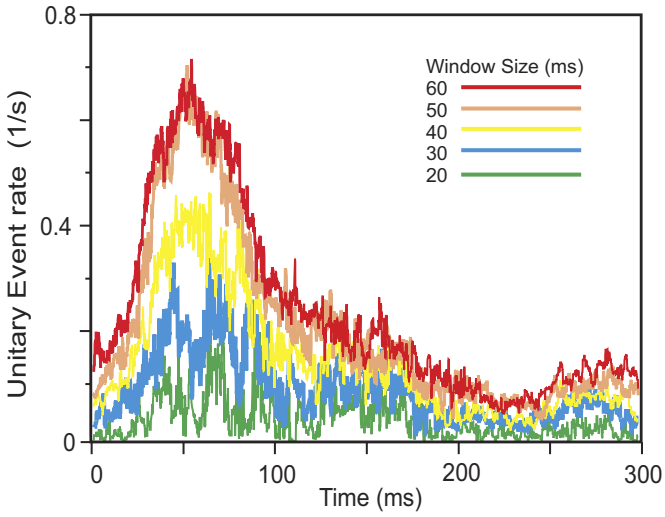

FIG. 7. UE profile as a function of analysis window width. Data were analyzed as for Fig. 4*G* for various analysis window widths (20 to 60 ms in 10-ms steps, color coded). The UE profiles exhibit an increasing maximum for increasing analysis window width, which is most strongly expressed for window size 40–60 ms. The peak height saturates for window sizes >50 ms. The peak of these curves is at the same point in time (50 ms after fixation onset).

Taken together, these controls indicate that the unitary event analysis applied here reliably detects the incidence and the time course of excess synchrony in nonstationary time series and ignores spurious, rate-dependent coincidences.

DISCUSSION

In contrast to previous studies (e.g., Vinje et al. 2000), we have not attempted to establish relations between eye movements and neuronal responses resulting from the passage of individual RFs over particular contours of the visual scene. Rather, we were interested in the relations between response variables such as discharge rate and spike synchronization during the various phases of visual scanning movements. Because our animals were free to direct their gaze to any location on the images, the actual stimulus for the cells changed with each saccade. Thus we measured the average behavior of cells under natural viewing conditions. We reasoned that this should allow us to detect characteristic, eye-movement–related response patterns and the results suggest that this was indeed the case. The application of multielectrode recordings revealed for the first time a fixation-related, transient increase of response synchronization. This increase in coincident firing is dissociated from the later increase in neuronal firing rate, suggesting that temporal coordination of discharges may play a role in the initial processing of signals in V1.

Methodological considerations

Because of the spike-sorting procedure that we applied to extract single-cell responses from the tetrode signals it is likely that we underestimated the incidence of synchronous firing. If cells recorded from the same tetrode discharge in precise synchrony, the respective spikes superimpose in a complex

way and are excluded from analysis (Gray et al. 1995). This limited our ability to detect synchronous firing of pairs of neurons recorded by the same tetrode and it also precluded detection of synchrony among cells recorded from different tetrodes if two cells recorded from one tetrode fired in precise synchrony with a third cell, recorded by another tetrode. Of a total of 1,369 pairs 262 were cells recorded from the same tetrode and 1,107 from distant electrodes. Thus we may have underestimated the incidence of synchronous firing by $\gtrsim$20%.

Functional implications

Several arguments suggest that the unexpectedly high incidence of synchronous firing was due to synchronizing neuronal interactions rather than a by-product of stimulus-induced covariation in firing rate. First, the statistical methods developed for the analysis of synchronous firing, the unitary event analysis, is specifically designed to eliminate spurious coincidences caused by joint rate increases. Second, the controls with dithering spike times provided independent evidence that the UEs were not due to rate covariations. Third, our simulations with artificially injected spikes showed that pure rate covariation could not explain the high incidence of UEs.

Interestingly, the phase of enhanced synchrony set in right at the beginning of the rate increases and reached its maximum 40 ms before the peak of the rate increase. Because UEs are virtually absent during saccades and because retinal response latencies cover a range of 30 to 60 ms, this implies that the synchronizing mechanism operates already and preferentially on the very first spikes evoked by the newly fixated parts of the image.

A mechanism capable of achieving such rapid synchronization has recently been identified (Fries et al. 2007). When the visual cortex is engaged in oscillatory activity in the gamma-frequency range, neurons in columns with related feature preferences oscillate in synchrony probably because of strong reciprocal connections between these columns. This has the effect that the onset latencies of responses to stimuli driving coherently oscillating columns become synchronized because they can fire only during the depolarizing phase of the oscillation cycles (Engel et al. 2001; Fries et al. 2001, 2007; see also Volgushev et al. 1998 for a related in vitro study). As a result this may lead to an increased synchronization of the very first spikes of responses to stimuli that match the preferences of synchronously oscillating columns.

A further mechanism suggesting that visually induced first spikes have a supportive role in synchronization, based on an internal, saccade-locked signal, was recently hypothesized. It was shown that there is a pronounced saccade-related, evoked local field potential (LFP) signal (Bartlett et al. 1976). This in turn could serve as a reference signal to realize the proposed amplitude-to-temporal code conversion suggested by Fries et al. (2007). Thus the saccade-evoked LFP would provide the reference frame for the timing of induced spikes and, in particular, would favor the first incoming spikes. There are first results supporting this hypothesis (Ito et al. 2008) that will be reported elsewhere.

For scene segmentation and object perception, stimulus features that share similarities tend to be bound together. Since neurons encoding related features engage in synchronous gamma oscillations, it has been proposed that these oscillations serve the translation of connectivity patterns into specific constellations of response synchronization that in turn support rapid feature-specific synchronization of discharges (Fries et al. 2001). This proposal is based on the evidence that precise synchronization of spikes selectively raises the saliency of the synchronized discharges and thereby favors their further joint processing (for review see Singer 1999). The rapid synchronization of spikes in the early postsaccadic fixation could thus be a reflection of such a temporal coding mechanism.

It has been concluded from measurements of recognition times that in V1 computations required for elementary scene analysis have to be accomplished within a few tens of milliseconds (Fabre-Thorpe et al. 2001). Because this allows for only a few spikes per neuron, it has been proposed that information should be encoded not only in the discharge rate but also in the precise temporal relations between the individual discharges of neurons. The present results support this scenario and suggest that the visual cortex possesses a mechanism to complement rate codes with a fast temporal coding strategy adjusting the timing of individual spikes. As suggested by the saccade-related occurrence of oscillatory activity, this precise synchronization could be due to saccade-related oscillatory activity of corollary origin. Several arguments make it appear likely that this corollary signal is related to mechanisms of attention. There is abundant evidence for a close relation between the mechanisms that control attention and saccadic eye movements, respectively (Corbetta et al. 1998; Everling 2007). Moreover, attentional mechanisms have been shown to modulate the oscillatory patterning of neuronal responses, which in turn modulates synchronous discharges. Focused attention and expectations are associated with an anticipatory entrainment of cortical networks in both beta and gamma oscillations (Fries et al. 2001; Roelfsema et al. 1997) and responses to attended stimuli exhibit stronger oscillatory patterning in the gamma-frequency range and stronger synchronization than responses to nonattended stimuli (Schoffelen et al. 2005; Steinmetz et al. 2000; Tiitinen et al. 1993). To further examine this possibility, field potential oscillation must be analyzed and related to the timing of spike discharges.

However, at this stage the possibility should not be dismissed that spike synchronization is caused in addition by retinal or thalamic mechanisms. There is evidence that the discharges of retinal ganglion cells are not independent and can become synchronized with millisecond precision in a stimulus-specific way (Meister et al. 1995; Neuenschwander et al. 1996). These synchronized volleys are transmitted with high temporal fidelity by the lateral geniculate nucleus (Castelo-Branco et al. 1998; Usrey and Reid 1999). Moreover, corticofugal projections to the lateral geniculate have been shown to have a synchronizing effect (Sillito et al. 1994). Both the retinal and the corticofugal synchronizing mechanisms induce coincident firing in neurons responding to continuous contours, suggesting the possibility that this early synchronization contributes to scene segmentation (Stephens et al. 2006). So far these synchronizations have been studied with stationary flashed or continuously moving contours. Therefore it is unknown whether the stimulation caused by the sudden arrest of rapidly moving contours, such as those occurring at the end of saccades, can induce such synchronization.

In conclusion, our data revealed that scanning of natural scenes is associated with a rapid succession of distinct fixation-related activation patterns that consist of a transient increase in excess coincident firing that is followed by a transient increase in discharge rate. This suggests the action of a fast-acting synchronizing mechanism that is in good agreement with the evidence that basic operations of scene analysis must be accomplished within a few tens of milliseconds in V1, most likely requiring temporal coding strategies.

ACKNOWLEDGMENTS

We thank the Chilean Primate Center—OMS Catholic University of Chile; C. M. Gray for useful comments on the manuscript; and M. Diesmann for clarifying discussions. Part of the work was performed while S. Grün was located at the Free University, Neuroinformatics, Institute for Biology (Neurobiology), Berlin, Germany.

GRANTS

This study was supported in part by Volkswagen Stiftung grants to P. Maldonado, W. Singer, and S. Grün; Iniciativa Científica Milenio Grant P04-068F, and a Stifterverband für die deutsche Wissenschaft grant to S. Grün.

REFERENCES

Bartlett JR, Doty RW, Lee BB, Sakakura H. Influence of saccadic eye movements on geniculostriate excitability in normal monkeys. *Exp Brain Res* 25: 487–509, 1976.

Buisseret P, Maffei L. Extraocular proprioceptive projections to the visual cortex. *Exp Brain Res* 28: 421–425, 1977.

Burr DC, Morrone MC, Ross J. Selective suppression of the magnocellular visual pathway during saccadic eye movements. *Nature* 371: 511–513, 1994.

Castelo-Branco M, Neuenschwander S, Singer W. Synchronization of visual responses between the cortex, lateral geniculate nucleus, and retina in the anesthetized cat. *J Neurosci* 18: 6395–6410, 1998.

Corbetta M, Akbudak E, Conturo TE, Snyder AZ, Ollinger JM, Drury HA, Linenweber MR, Petersen SE, Raichle ME, Van Essen DC, Shulman GL. A common network of functional areas for attention and eye movements. *Neuron* 21: 761–773, 1998.

Date A, Bienenstock E, Geman S. *On the Temporal Resolution of Neural Activity* (Technical report). Providence, RI: Brown Univ., Division of Applied Mathematics, 1998.

Engel AK, Fries P, Singer W. Dynamic predictions: oscillations and synchrony in top-down processing. *Nat Rev Neurosci* 2: 704–716, 2001.

Everling S. Where do I look? From attention to action in the frontal eye field. *Neuron* 56: 417–419, 2007.

Fabre-Thorpe M, Delorme A, Marlot C, Thorpe S. A limit to the speed of processing in ultra-rapid visual categorization of novel natural scenes. *J Cogn Neurosci* 13: 171–180, 2001.

Friedman-Hill S, Maldonado PE, Gray CM. Dynamics of striate cortical activity in the alert macaque: I. Incidence and stimulus-dependence of gamma-band neuronal oscillations. *Cereb Cortex* 10: 1105–1116, 2000.

Fries P, Nikolic D, Singer W. The gamma cycle. *Trends Neurosci* 30: 309–316, 2007.

Fries P, Reynolds JH, Rorie AE, Desimone R. Modulation of oscillatory neuronal synchronization by selective visual attention. *Science* 291: 1560–1563, 2001.

Gerstein GL. Searching for significance in spatio-temporal firing patterns. *Acta Neurobiol Exp* (*Wars*) 64: 203–207, 2004.

Gray CM, Maldonado PE, Wilson M, McNaughton B. Tetrodes markedly improve the reliability and yield of multiple single-unit isolation from multi-unit recordings in cat striate cortex. *J Neurosci Methods* 63: 43–54, 1995.

Grün S, Diesmann M, Aertsen A. Unitary events in multiple single-neuron spiking activity: I. Detection and significance. *Neural Comput* 14: 43–80, 2002a.

Grün S, Diesmann M, Aertsen A. Unitary events in multiple single-neuron spiking activity: II. Nonstationary data. *Neural Comput* 14: 81–119, 2002b.

Grün S, Diesmann M, Grammont F, Riehle A, Aertsen A. Detecting unitary events without discretization of time. *J Neurosci Methods* 94: 67–79, 1999.

Grün S, Riehle A, Diesmann M. Effect of cross-trial nonstationarity on joint-spike events. *Biol Cybern* 88: 335–351, 2003.

Guyonneau R, Vanrullen R, Thorpe SJ. Temporal codes and sparse representations: a key to understanding rapid processing in the visual system. *J Physiol* (*Paris*) 98: 487–497, 2004.

Hopfield JJ. Encoding for computation: recognizing brief dynamical patterns by exploiting effects of weak rhythms on action-potential timing. *Proc Natl Acad Sci USA* 101: 6255–6260, 2004.

Ito J, Maldonado P, Grün S. Saccade-related LFP oscillations set the stage for processing visually evoked spikes (Abstract I-ll). *Computational and Systems Neuroscience* (COSYNE) 2008, Salt Lake City, UT.

Jones HE, Grieve KL, Wang W, Sillito AM. Surround suppression in primate V1. *J Neurophysiol* 86: 2011–2028, 2001.

Judge SJ, Richmond BJ, Chu FC. Implantation of magnetic search coils for measurement of eye position: an improved method. *Vision Res* 20: 535–538, 1980.

McAdams CJ, Maunsell JH. Effects of attention on orientation-tuning functions of single neurons in macaque cortical area V4. *J Neurosci* 19: 431–441, 1999.

Meister M, Lagnado L, Baylor DA. Concerted signaling by retinal ganglion cells. *Science* 270: 1207–1210, 1995.

Nawrot MP, Boucsein C, Rodriguez Molina V, Riehle A, Aertsen A, Rotter S. Measurement of variability dynamics in cortical spike trains. *J Neurosci Methods* 169: 374–390, 2008.

Neuenschwander S, Singer W. Long-range synchronization of oscillatory light responses in the cat retina and lateral geniculate nucleus. *Nature* 379: 728–733, 1996.

Pazienti A, Diesmann M, Grün S. Bounds of the ability to destroy precise coincidences by spike dithering. In: *Advances in Brain, Vision, and Artificial Intelligence* (Lecture Notes in Computer Science). Berlin: Springer Berlin/Heidelberg, 2007, vol. 4729, p. 428–437.

Pazienti A, Maldonado PE, Diesmann M, Grün S. The effectiveness of systematic spike dithering depends on the precision of cortical synchronization. *Brain Res* 1225, 39–46, 2008.

Pipa G, van Vreeswijk C, Grün S. Auto-structure of spike-trains matters for testing on synchronous activity (Abstract II-38). Computational and Systems Neuroscience (COSYNE) 2008, Salt Lake City, UT.

Purpura KP, Kalik SF, Schiff ND. Analysis of perisaccadic field potentials in the occipitotemporal pathway during active vision. *J Neurophysiol* 90: 3455–3478, 2003.

Riehle A, Grün S, Diesmann M, Aertsen A. Spike synchronization and rate modulation differentially involved in motor cortical function. *Science* 278: 1950–1953, 1997.

Roelfsema PR, Engel AK, König P, Singer W. Visuomotor integration is associated with zero time-lag synchronization among cortical areas. *Nature* 385: 157–161, 1997.

Schoffelen JM, Oostenveld R, Fries P. Neuronal coherence as a mechanism of effective corticospinal interaction. *Science* 308: 111–113, 2005.

Shmiel T, Drori R, Shmiel O, Ben-Shaul Y, Nadasdy Z, Shemesh M, Teicher M, Abeles M. Temporally precise cortical firing patterns are associated with distinct action segments. *J Neurophysiol* 96: 2645–2652, 2006.

Sillito AM, Jones HE, Gerstein GL, West DC. Feature-linked synchronization of thalamic relay cell firing induced by feedback from the visual cortex. *Nature* 369: 479–482, 1994.

Singer W. Neuronal synchrony: a versatile code for the definition of relations? *Neuron* 24: 49–25, 1999.

Steinmetz PN, Roy A, Fitzgerald PJ, Hsiao SS, Johnson KO, Niebur E. Attention modulates synchronized neuronal firing in primate somatosensory cortex. *Nature* 404: 187–190, 2000.

Stephens GJ, Neuenschwander S, George JS, Singer W, Kenyon GT. See globally, spike locally: oscillations in a retinal model encode large visual features. *Biol Cybern* 95: 327–348, 2006.

Sugita Y. Grouping of image fragments in primary visual cortex. *Nature* 401: 269–272, 1999.

Tiitinen H, Sinkkonen J, Reinikainen K, Alho K, Lavikainen J, Naatanen R. Selective attention enhances the auditory 40-Hz transient response in humans. *Nature* 364: 59–60, 1993.

Trotter Y, Celebrini S. Gaze direction controls response gain in primary visual-cortex neurons. *Nature* 398: 239–242, 1999.

Usrey WM, Reid RC. Synchronous activity in the visual system. *Annu Rev Physiol* 61: 435–456, 1999.

Vinje WE, Gallant JL. Sparse coding and decorrelation in primary visual cortex during natural vision. *Science* 287: 1273–1276, 2000.

Volgushev M, Chistiakova M, Singer W. Modification of discharge patterns of neocortical neurons by induced oscillations of the membrane potential. *Neuroscience* 83: 15–25, 1998.